

Characterizing The Many-Body Localization by Studying State Sensitivity to Boundary Conditions

Mohammad Pouranvari

*Department of Physics, Faculty of Basic Sciences,
University of Mazandaran, P. O. Box 47416-95447, Babolsar, Iran*

Shiuan-Fan Liou

Private sector

(Dated: August 11, 2020)

We introduce novel characterizations for many body phase transitions between delocalized and localized phases based on the system's sensitivity to the boundary conditions. In particular, we change single-particle boundary conditions from periodic to antiperiodic and calculate shift in the system's energy and shifts in the single-particle density matrix eigenvalues in the corresponding energy window. We employ the typical model for studying MBL, a one-dimensional disordered system of fermions with nearest-neighbor repulsive interaction where disorder is introduced as randomness on on-site energies. By calculating the shifts numerically in the system's energy and eigenvalues of the single-particle density matrix, we observe that in the localized regime, both shifts are vanishing; while in the extended regime, the shifts are significant. We also applied these characterizations of the phase transition to the case of having next-nearest-neighbor interactions in addition to the nearest-neighbor interactions, and studied its effect on the transition.

I. INTRODUCTION

In a free fermion model with the extending plain-wave eigenfunctions, fermions move freely in the entire system. Introducing randomness in the free fermion model, which represents impurities, leads to the localization of fermions due to the quantum interference by heavy impurities, proposed by Anderson¹. This phenomenon, so-called Anderson localization, has been widely studied numerically, analytically, and experimentally. In general, the Anderson localization is associated with the symmetry and dimension of the system². For one- and two-dimensional systems, any infinitesimal uncorrelated randomness makes them localized³. For a three-dimensional (3D) system, however, there exists a non-zero critical disorder strength⁴ at which a quantum phase transition between localized and delocalized phases occurs. In a weak randomness regime, the system can still be delocalized; as the impurity strength increases and hits the critical value, it becomes localized. Besides, a phase transition from a delocalized to a localized phase can also be seen in the energy resolution, if the system under study has mobility edges. A 3D Anderson model, for example, has localized phases at both tails of the energy spectrum, and delocalized phases in the middle of the spectrum^{5,6}. Thus, as the system's energy changes from one energy window to another, it will undergo a phase transition between localized and delocalized phases.

Another interesting phenomenon arises when an interaction is introduced in the Anderson model, whence we encounter the following questions: Will interactions suppress the effect of the impurity, or the impurity effect is so strong that makes the interacting system localized? More interestingly, what role does temperature play in such a system? We can also ask these questions from the perspective of statistical physics: It is assumed that an

ergodic system can visit its whole phase space after a finite time, so the averaging an observable over time is the same as averaging over the whole phase space. In this perspective, the question of the ergodicity of a random interacting system is important⁷. Answering the above questions is one of the hot research topics. By now, we know that in the interacting systems, at non-zero temperature, a phase transition between localized and delocalized phases arises from varying disorder strength. With strong disorders, the conductivity— even at a non-zero temperature— is zero, and the state of the system is localized in Fock space. The phase is thus called many-body localized (MBL) phase^{8–13}. The states in the MBL phase do not thermalize in the sense that after a long time, its properties still depend on the initial state of the system (i.e. local integrals of motion constrain the system); in other words, the system carries the information of the initial states. Thus, an MBL phase is an out-of-equilibrium phase, and the laws of statistical mechanics are not obeyed. On the other hand, with weak disorders, a part of the system acts as a bath for the remainder, such that the eigenstate thermalization hypothesis (ETH)^{14–17} can be applied, and the system thermalizes. In addition, an ETH-MBL phase transition can be seen at a fixed disorder strength in the energy resolution, i.e. the mobility edges can also be seen in the interacting system. The transition from ETH to the MBL phase is not a thermodynamic phase transition, and the exclusion of the phase transition at a non-zero temperature is not relevant here. Instead, it is a dynamical phase transition^{18,19}: a universal class of non-equilibrium phenomena, where a phase transition happens as time goes on.

Experimentally, phase transition between the ETH and MBL phases have been witnessed in many fields and systems such as ultra-cold atoms²⁰, trapped ions systems²¹, optical lattices^{22–28}, and quantum informa-

tion systems²⁹.

The typical model employed to study the ETH-MBL phase transition is the Jordan-Wigner transformation of the XXZ model for the spin 1/2 which is the spinless fermion model with constant nearest-neighbor (NN) hopping and NN interactions; randomness is introduced by random on-site energies. Some studies^{30–32} even introduce random interactions into the system. The relations between the MBL effect and the localization of single-particle states and single-particle translation-invariant have been investigated^{32–35}. Although impurities are usually described by random on-site energies, some studies reported that on-site energies with incommensurate periodicity^{36–38} could trigger ETH-MBL phase transitions; without impurities, other systems such as a frustrated spin chain³⁹ and a system under strong electric field⁴⁰ also exhibit ETH-MBL phase transitions. Although we expect extended systems to be ergodic, some works claim that there is an extended but non-ergodic phase in ETH phase^{36,38,41,42}.

Finding a Characterization for the ETH-MBL phase transition is part of the current research. EE is one candidate that shows distinguished behavior in the ETH and MBL phases^{43,44}. EE follows an area law behavior in the MBL phase, although there is no transport^{45,46}. However, since the reduced density matrix of a subsystem approaches the thermal density matrix in the ETH phase, EE obeys volume law. EE thus fluctuates strongly around the localization-delocalization transition point. A detailed study of the transition from MBL to ETH phase⁴⁷ found that entanglement entropy behaves sub-thermal in the quantum critical regime. Besides, the variance of the entanglement from sample to sample, intra-sample, and for different eigenstates were also investigated as a characterization of the phase transition. The statistics of the low energy entanglement spectrum, which goes from Gaussian orthogonal ensemble in extended regime to a Poisson distribution in localized regime⁴¹, has been a study subject as well. Furthermore, people have been interested in the statistics of the level spacing of eigen-energies⁴⁸. Some fancy methods, such as machine learning is also used for detecting the MBL phase transition⁴⁹.

A recent paper⁵⁰ studied the single-particle density matrix to distinguish MBL from the ETH phase. The single-particle density matrices are constructed by the eigenstates of the Hamiltonian (H) of the system in a target energy window through

$$\rho_{ij} = \langle \psi | c_i^\dagger c_j | \psi \rangle, \quad (1)$$

where i and j go from 1 to L , system size, and $|\psi\rangle$ is the eigenstate of the H . They studied eigenvalues $\{n\}$ and eigenfunctions of the density matrix. Its eigenvalues, which can be interpreted as occupations of the orbitals, demonstrate the Fock space localization. Deep in the delocalized phase, $\{n\}$'s are evenly spaced between 0 and 1. While, in the localized phase, they tend to be very close to either 0 or 1. Thus, the difference between

two consecutive eigenvalues of ρ shows different behavior in delocalized and localized phases. Moreover, they found that eigenfunctions $|\phi_k\rangle$ of the density matrix, are extended (localized) in delocalized (MBL) phase^{51,52}.

We, in this paper, look at the ETH-MBL phase transition from the perspective of boundary condition effects on the system, namely, we change the single-particle boundary conditions from periodic to antiperiodic and then study its effects on the system's energy as well as on the eigenvalues of the single-particle density matrix (ρ) at a given energy window (see section II for more detail). We found that the system's energy and occupation numbers are sensitive to the boundary conditions in the ETH phase. In MBL phase, however, the change in boundary condition has a negligible effect on them. We test this idea in a previously studied model with NN interactions that have a known ETH-MBL phase transition. We also apply our characterization method to a model having both NN and NNN interactions.

The paper's structure is as follows; We first introduce the model and explain the numerical method in section II. The responses of the Hamiltonian's eigen-energy and the single-particle density matrix to the boundary conditions, considering only the NN interaction, will be presented in sections III and IV, respectively. In sec V, we introduce the NNN interaction in the model and consider its effect. In the end, we close with some remarks and suggested works in section VI.

II. METHOD AND MODEL

We consider spinless fermions confined on a one-dimensional (1D) chain with the nearest-neighbor (NN) hopping; NN and next-nearest-neighbor (NNN) repulsive density-density interactions as well as diagonal disorders. The effective Hamiltonian can be written as:

$$H = -t \sum_{i=1}^L (c_i^\dagger c_{i+1} + h.c.) + \sum_{i=1}^L \mu_i (n_i - \frac{1}{2}) + V_1 \sum_{i=1}^L (n_i - \frac{1}{2})(n_{i+1} - \frac{1}{2}) + V_2 \sum_{i=1}^L (n_i - \frac{1}{2})(n_{i+2} - \frac{1}{2}). \quad (2)$$

where $c_i^\dagger (c_i)$ is the fermionic creation (annihilation) operator, creating (annihilating) a fermion on the site i and $n_i = c_i^\dagger c_i$ is the number operator. The first term in the Hamiltonian is the NN hopping with constant strength t , which is used as the energy unit in our calculations and is set to unity. The randomized on-site energies representing disorders are described by μ 's, which obey the uniform distribution within $[-W, W]$, where W is called disorder strength. The last two terms are the constant repulsive NN and NNN density-density interactions.

To apply boundary conditions, we set $c_{i+L}^{(\dagger)} = c_i^{(\dagger)}$ for the the periodic boundary condition (PBC) and $c_{i+L}^{(\dagger)} =$

$-c_i^{(\dagger)}$ for the antiperiodic boundary condition (APBC) where L is the length of the 1D chain.

We first diagonalize the Hamiltonian through exact diagonalization method, and find its eigenvectors and the corresponding eigenvalues. We use the parameter $\epsilon = \frac{(E-E_0)}{(E_{max}-E_0)}$, where E is the target energy, E_0 is the ground state energy, and E_{max} represents the highest energy in the spectrum; it changes between 0 and 1 corresponding to the ground state and highest energy, respectively. We focus on a certain energy window of the spectrum: For a given ϵ , we calculate the target energy E and select six eigenstates of H with the energy closest to E . For each of these six eigenstates, we build up the single-particle density matrix ρ from Eq. (1). By changing the boundary conditions from PBC to APBC, we calculate the energy shift for each eigenstate:

$$\delta E_i = |E_{i,PBC} - E_{i,APBC}|, \quad (3)$$

where E_i is the energy of the i th eigenstate. We then take typical averaging over six eigenstates and take typical disorder average to obtain δE^{typ} . In the same manner, we calculate shifts in the eigenvalues of the single-particle density matrix:

$$\delta n_i^{(j)} = |n_{i,PBC}^{(j)} - n_{i,APBC}^{(j)}|. \quad (4)$$

A typical average on all eigenvalues of the ρ (j goes from 1 to L), another typical average over the six samples, and a typical disorder average will be calculated to obtain δn^{typ} .

III. EFFECT OF THE SINGLE-PARTICLE BOUNDARY CHANGE ON THE ENERGY

In a free fermion model, the state of the system is the Slater determinant of the occupied single-particle eigenstates. In the localized phase, occupied eigenstates of the system are localized in a small region of space, while in the delocalized phase, they are extended. In Ref. [53], the effect of the change in the boundary conditions on the single-particle eigen-energies of a free fermion model is studied. By changing the boundary conditions in the localized phase, the single-particle energy does not change. On the other hand, in the delocalized phase, where eigenstates of the system are extended, any changes in the boundary conditions can be seen by the wave-function; these changes are then reflected in the corresponding energy shifts. Accordingly, the energy shift for each level, δE , divided by the average level spacing ΔE known as Thouless conductance, is a characterization of the Anderson phase transition between delocalized and localized phases:

$$g_E = \delta E / \Delta E. \quad (5)$$

On the other hand, we know that for an interacting model, states of the system is localized (delocalized) in

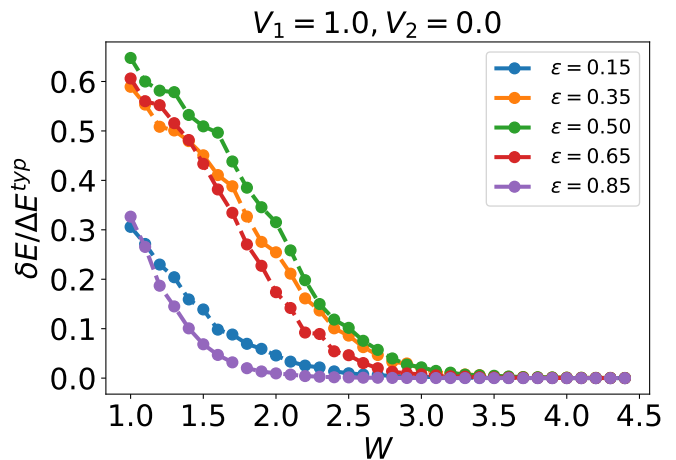


FIG. 1. (color online) typical averaged $g_E = \frac{\delta E}{\Delta E}$ for the case of having only NN interaction ($V_1 = 1, V_2 = 0$) for some selected ϵ as disorder strength W varies. We set $L = 14, N = 7$. We take typical disorder average over altogether 2000 samples for each data point.

the *Fock space* for localized (extended) phase; i.e. in the localized phase, only N (number of fermions) of the single-particle eigenstates make the state of the system, while in the delocalized phase all the eigenstates have a contribution to the state. Thus, we conjecture that if we change boundary conditions, we can use a similar quantity as Thouless conductance (now for the system's energy rather than the single-particle eigen-energy) to characterize the phase transition. In particular, we change the single-particle boundary condition from periodic to antiperiodic (as explained in section II) and calculate g_E for the system's energy. In Fig. 1, typical averaged g_E is plotted for some selected values of the energy for the case of NN interaction of Eq. (2) corresponding to $V_1 = 1, V_2 = 0$. In the averaging over random samples, we take typical average rather than arithmetic average to consider very small values. We see that deep in the delocalized phase, this shift is on the order of 1, while deep in the localized phase, the shift is negligible. Based on this plot, in the middle of the spectrum ($\epsilon = 0.5$), g_E goes to zero at $W \approx 3.5$, consistent with the previously obtained results^{54–57}. Also, g_E is plotted for the whole spectrum of energy in Fig. 2 as we vary the disorder strength W . This plot is also consistent with the previously obtained results.

IV. EFFECT OF THE SINGLE-PARTICLE BOUNDARY CHANGE ON THE SINGLE-PARTICLE DENSITY MATRIX

Now, we focus on the effect of boundary conditions on the occupation numbers of density matrix Eq. (1). First, let us look at the case of free fermions, where we

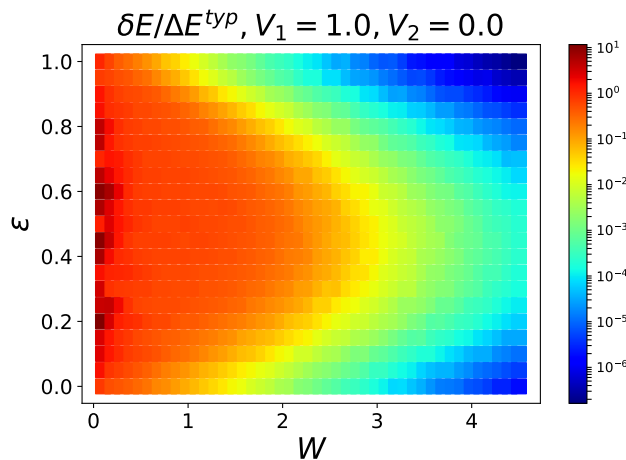


FIG. 2. (color online) typical average of $g_E = \frac{\delta E}{\Delta E}^{\text{typ}}$ for the entire spectrum of the energy as we change the disorder strength W for the NN interaction case ($V_1 = 1, V_2 = 0$). System size $L = 14, N = 7$. We take typical disorder average over altogether 2000 samples for each data point.

can write the Hamiltonian of the system as:

$$H = \sum_{i,j=1}^L h_{i,j} c_i^\dagger c_j, \quad (6)$$

we observe that eigen-functions of the single-particle density matrix and single-particle matrix h are the same:

$$\rho|\phi_k\rangle = n_k|\phi_k\rangle, \quad (7)$$

$$h|\phi_k\rangle = \epsilon_k|\phi_k\rangle, \quad (8)$$

where ϵ_k is the single-particle eigen-energy of the Hamiltonian. With the argument of the Thouless⁵³, eigenvalues of the single-particle density matrix are sensitive (insensitive) to the boundary conditions in delocalized (localized) phases. Thus, we can identify the shifts in the eigenvalues of the single-particle density matrix when we change the boundary condition from periodic to antiperiodic as a probe of the phase transition. This idea has been verified before indirectly: Effect of the boundary condition changes on the entanglement Hamiltonian for free fermion models was studied in Ref [58], where boundary condition is changed from periodic to antiperiodic and shifts in the eigenvalues of the entanglement Hamiltonian (and thus on the entanglement entropy) are calculated. Note that entanglement Hamiltonian of a subsystem is obtained from single-particle density matrix of the corresponding subsystem for the free fermion case. It is shown that the shifts in the entanglement Hamiltonian eigenvalues thus shift in the entanglement entropy characterizing the localized-delocalized phases transition.

For the interacting case, we know that the single-particle density matrix eigenstates are localized (delocalized) in the localized (delocalized) phase⁵⁰; Thus, we put one forward step and conjecture that ETH phase

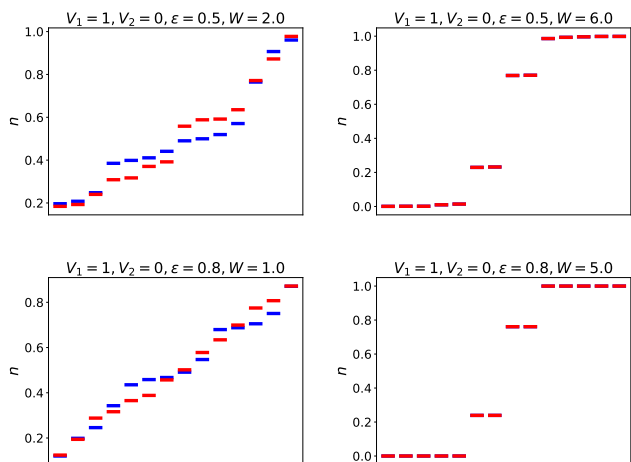


FIG. 3. (color online) eigenvalues of the single-particle density matrix (occupation numbers $\{n\}$) corresponding to periodic boundary condition (Blue), and antiperiodic boundary condition (red) for NN interaction of Eq.(2) ($V_1 = 1, V_2 = 0$). In left plots, ϵ and W are chosen such that we are in the extended phase, while in the right plots, they correspond to the MBL phase. We set $L = 14, N = 7$. Only one sample is considered, and we do not take disorder average. We see that shifts in the occupation numbers in the MBL phase are almost zero, while the shifts are appreciable in the extended phase.

can be distinguished from the MBL phase by analyzing the shifts of the occupation numbers when we change boundary conditions. In particular, we change the single-particle boundary condition from periodic to antiperiodic (as described in Section II) and calculate the shifts in the occupation numbers of single-particle density matrix δn .

In Fig. 3 we plot occupation numbers for the NN interaction of Eq. (2) corresponding to $V_1 = 1, V_2 = 0$, for single-particle periodic and antiperiodic boundary conditions in extended and MBL phases. Here just one sample is considered without disorder averaging. We can see that in the MBL phase, occupation numbers corresponding to PBC and APBC are almost identical, and the shifts are negligible; in contrast, we get a non-vanishing change of the occupation numbers in the extended phase. The interpretation of these results is the followings: In the localized phase, where just a fraction of the single-particle eigenstates contribute to the state of the system, by changing the boundary conditions, filled/empty single-particle eigenstates remain untouched. On the other hand, in the delocalized phase, the non-zero contribution of all the single-particle eigenstates changes; some drop their contributions, and others gain more.

To have a characterization independent of the system size, we divide δn to average level spacing for occupation numbers, Δn , and introduce the following as an ETH-MBL phase transition characterization:

$$g_n = \delta n / \Delta n. \quad (9)$$

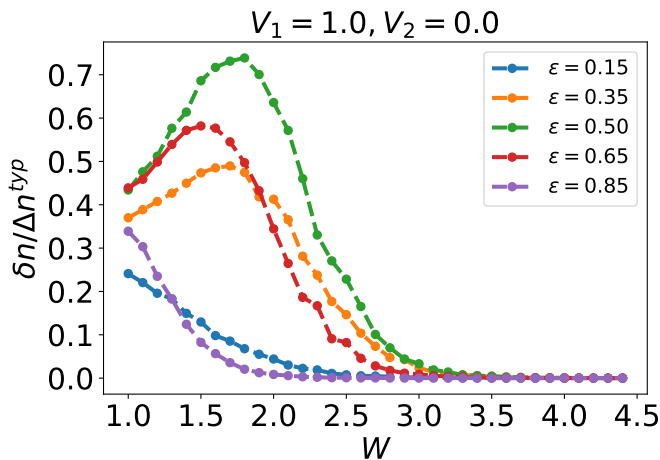


FIG. 4. (color online) typical averaged $g_n = \frac{\delta n}{\Delta n}$ for the NN interaction case of Eq. (2) corresponding to $V_1 = 1, V_2 = 0$, for some selected values of ϵ 's, as we change the disorder strength W . At large values of ϵ , g_n goes to zero faster than small values of ϵ . We set $L = 14, N = 7$. We take typical average over altogether 2000 samples for each data point.

We plot typical averaged $\frac{\delta n}{\Delta n}$ for the NN case of Eq. (2) ($V_1 = 1, V_2 = 0$) for some selected values of ϵ , as we change disorder strength W in Fig. 4. We see that, g_n is non-zero in the delocalized phase for each energy, and it vanishes in the localized phase. In the middle of the spectrum ($\epsilon = 0.5$), we obtain $W_c \approx 3.6$, consistent with the previously obtained results^{54–57}. We see that g_n is not symmetric to the middle of the spectrum; it is tilted toward smaller densities; i.e. at large energy densities, states become localized easier than states at smaller energy densities; this is also consistent with the previous results.

By looking at g_n , we can also observe mobility edges, the points in the energy spectrum where phase changes between the delocalized and localized for a fixed value of disorder strength. We calculate g_n for a fixed value of W , as we change ϵ . The results are plotted in Fig. 5. We see that for $W = 1.0$, g_n is non-zero, while for $W = 4.5$ it vanishes for all values of ϵ and thus, there are no mobility edges for both cases. For other disorder strength, we can see mobility edges where g_n goes to zero. All this information can be summarized in Fig. 6, where g_n is calculated for the entire energy spectrum as we change disorder strength W .

V. NEAREST-NEIGHBOR AND NEXT-NEAREST-NEIGHBOR INTERACTIONS

It is also instructive to apply our method of characterizing ETH-MBL phase transition to the case of having both NN and NNN interactions, corresponds to $V_1 = 1, V_2 = 1$ in Eq. (2). Having NNN interaction in addition to the NN interaction makes localization harder;

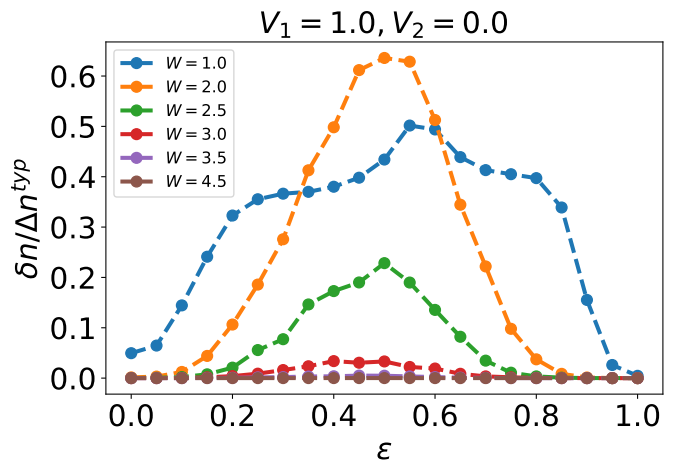


FIG. 5. (color online) typical averaged $g_n = \frac{\delta n}{\Delta n}$ for the NN interaction case of Eq. (2) corresponding to $V_1 = 1, V_2 = 0$, for some selected values of disorder strength W , as energy varies. We set $L = 14, N = 7$. We take typical average over altogether 2000 samples for each data point.

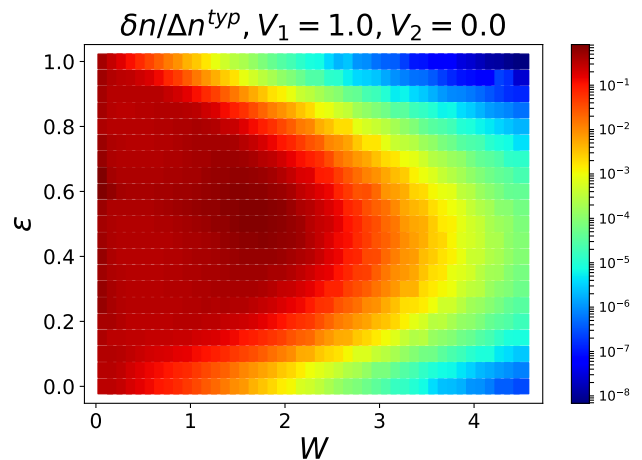


FIG. 6. (color online) typical averaged $g_n = \frac{\delta n}{\Delta n}$ for the NN interaction case of Eq. (2) corresponding to $V_1 = 1, V_2 = 0$, for the entire energy spectrum as we change the disorder strength W . We set $L = 14, N = 7$. We take typical average over altogether 2000 samples for each data point.

i.e. we expect that a larger amount of disorder is required to make the state localized for each energy spectrum and thus transition from ETH to MBL happens at a larger value of W_c compare to the NN case. Obtained results of g_E and g_n for the case of $V_1 = 1, V_2 = 1$ are plotted in Figs. 7 and 8. As we expect, localization becomes harder. We also see that the transition point becomes more asymmetric compare to the NN case. Moreover, there is no phase transition between ETH and MBL for states with the largest ϵ 's, and those states are localized with a non-zero disorder strength.

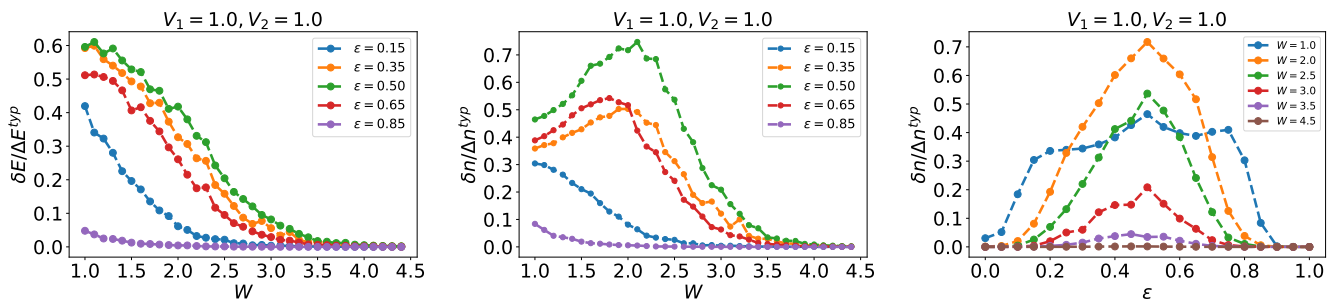


FIG. 7. (color online) left panel: typical averaged $g_E = \frac{\delta E}{\Delta E}$ for the case of having both NN and NNN interactions corresponding to $V_1 = 1, V_2 = 1$ in Eq. (2) for some specific ϵ 's as disorder strength W varies. We can see that for larger ϵ 's, g_E vanishes at a lower value of disorder strength, compared to the smaller ϵ 's. Middle panel: behavior of the typical disorder averaged $g_n = \frac{\delta n}{\Delta n}$ for the case of NN and NNN interactions for some selected values of ϵ 's, as we change the disorder strength W . We see similar behavior as the left panel. Right panel: typical averaged $g_n = \frac{\delta n}{\Delta n}$ for the case of NN and NNN interactions for some selected values of disorder strength W as energy varies, where we can see the mobility edges. For all plots, We set $L = 14, N = 7$. We take typical average over altogether 2000 samples for each data point.

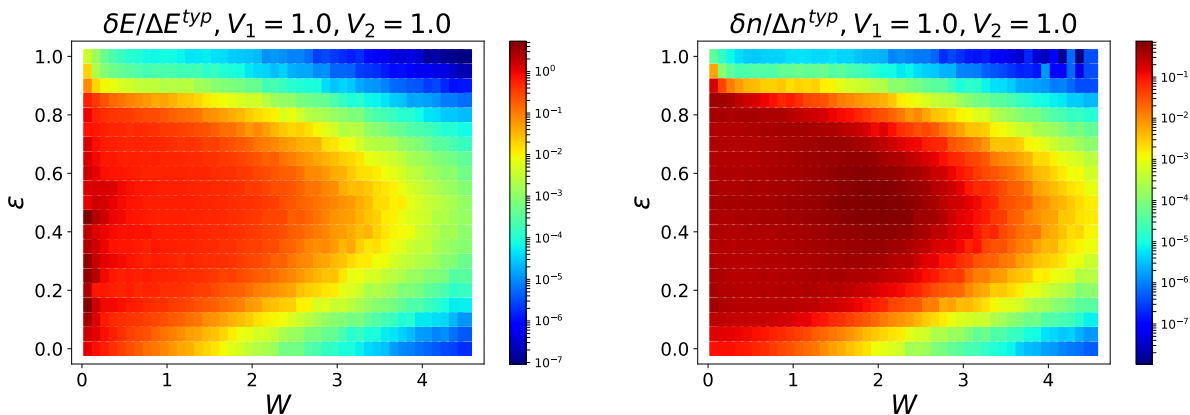


FIG. 8. (color online) left panel: typical average of $g_E = \frac{\delta E}{\Delta E}$ for the entire spectrum of the energy as we change the disorder strength W for the case of having both NN and NNN interactions corresponding to $V_1 = 1, V_2 = 1$ in Eq. (2). Right panel: typical averaged $g_n = \frac{\delta n}{\Delta n}$ in the same model for the entire energy as we change the disorder strength W . We set $L = 14, N = 7$. We take typical average over altogether 2000 samples for each data point.

VI. CONCLUSION AND OUTLOOK

Regarding the ETH-MBL phase transition in random interacting systems, finding the phase characterizations are one of main research today. In this work, we introduced new methods for characterizing the phase transition; namely, we studied the response of the system to the boundary conditions. For free fermions, the effect of change in boundary conditions on single-particle eigen-energies⁵³, as well as on the single-particle density matrix⁵⁸ has been studied before. Extended eigenstates feel what happens at the boundary, while changes in boundary conditions are not reflected in the localized phase. We extend this idea to the interacting case. In particular, we changed the single-particle boundary conditions between periodic and antiperiodic; then, we stud-

ied the echo of these changes in the energy of the system and the eigenvalues of the single-particle density matrix. We applied these characterizations to the 1D interacting model with randomness, a model that has been studied before, and we know approximately the phase transition point. We could identify the ETH phase with significant shifts in the system's energy and significant shifts in the occupation numbers. In contrast, the MBL phase has a vanishing response to the change in the boundary conditions. Furthermore, we added extra NNN interactions and studied its effects on the ETH-MBL phase transition.

ACKNOWLEDGMENTS

This work was supported by the Iran National Science Foundation (INSF) and the University of Mazandaran (M. P.).

- ¹ P. W. Anderson, *Phys. Rev.* **109**, 1492 (1958).
- ² R. Horodecki, P. Horodecki, M. Horodecki, and K. Horodecki, *Rev. Mod. Phys.* **81**, 865 (2009).
- ³ F. Evers and A. D. Mirlin, *Rev. Mod. Phys.* **80**, 1355 (2008).
- ⁴ A. MacKinnon and B. Kramer, *Phys. Rev. Lett.* **47**, 1546 (1981).
- ⁵ E. N. Economou and M. H. Cohen, *Phys. Rev. B* **5**, 2931 (1972).
- ⁶ F. M. Izrailev and A. A. Krokhin, *Phys. Rev. Lett.* **82**, 4062 (1999).
- ⁷ R. Nandkishore and D. A. Huse, *Annual Review of Condensed Matter Physics* **6**, 15 (2015), <https://doi.org/10.1146/annurev-conmatphys-031214-014726>.
- ⁸ D. Basko, I. Aleiner, and B. Altshuler, *Annals of Physics* **321**, 1126 (2006).
- ⁹ E. Altman, *Nature Physics* **14**, 979 (2018).
- ¹⁰ D. A. Abanin, E. Altman, I. Bloch, and M. Serbyn, *Rev. Mod. Phys.* **91**, 021001 (2019).
- ¹¹ S. A. Parameswaran, A. C. Potter, and R. Vasseur, *Annalen der Physik* **529**, 1600302 (2017), <https://onlinelibrary.wiley.com/doi/pdf/10.1002/andp.201600302>(2015).
- ¹² F. Alet and N. Laflorencie, *Comptes Rendus Physique* **19**, 498 (2018), quantum simulation / Simulation quantique.
- ¹³ E. Altman and R. Vosk, *Annual Review of Condensed Matter Physics* **6**, 383 (2015), <https://doi.org/10.1146/annurev-conmatphys-031214-014701>.
- ¹⁴ J. M. Deutsch, *Phys. Rev. A* **43**, 2046 (1991).
- ¹⁵ M. Srednicki, *Phys. Rev. E* **50**, 888 (1994).
- ¹⁶ M. Rigol, V. Dunjko, and M. Olshanii, *Nature* **452**, 854 EP (2008).
- ¹⁷ J. M. Deutsch, *Reports on Progress in Physics* **81**, 082001 (2018).
- ¹⁸ M. Heyl, *Reports on Progress in Physics* **81**, 054001 (2018).
- ¹⁹ A. A. Zvyagin, *Low Temperature Physics* **42**, 971 (2016), <https://doi.org/10.1063/1.4969869>.
- ²⁰ I. Bloch, J. Dalibard, and W. Zwerger, *Rev. Mod. Phys.* **80**, 885 (2008).
- ²¹ J. Smith, A. Lee, P. Richerme, B. Neyenhuis, P. W. Hess, P. Hauke, M. Heyl, D. A. Huse, and C. Monroe, *Nature Physics* **12**, 907 EP (2016).
- ²² T. Langen, R. Geiger, and J. Schmiedmayer, *Annual Review of Condensed Matter Physics* **6**, 201 (2015), <https://doi.org/10.1146/annurev-conmatphys-031214-014548>.
- ²³ C. Chin, R. Grimm, P. Julienne, and E. Tiesinga, *Rev. Mod. Phys.* **82**, 1225 (2010).
- ²⁴ A. M. Kaufman, M. E. Tai, A. Lukin, M. Rispoli, R. Schittko, P. M. Preiss, and M. Greiner, *Science* **353**, 794 (2016), <http://science.sciencemag.org/content/353/6301/794.full.pdf>.
- ²⁵ P. Bordia, H. Lüschen, U. Schneider, M. Knap, and I. Bloch, *Nature Physics* **13**, 460 EP (2017), article.
- ²⁶ J.-y. Choi, S. Hild, J. Zeiher, P. Schauß, A. Rubio-Abadal, T. Yefsah, V. Khemani, D. A. Huse, I. Bloch, and C. Gross, *Science* **352**, 1547 (2016), <http://science.sciencemag.org/content/352/6293/1547.full.pdf>.
- ²⁷ P. Bordia, H. P. Lüschen, S. S. Hodgman, M. Schreiber, I. Bloch, and U. Schneider, *Phys. Rev. Lett.* **116**, 140401 (2016).
- ²⁸ M. Schreiber, S. S. Hodgman, P. Bordia, H. P. Lüschen, M. H. Fischer, R. Vosk, E. Altman, U. Schneider, and I. Bloch, *Science* **349**, 842 (2015), <http://science.sciencemag.org/content/349/6250/842.full.pdf>.
- ²⁹ L. Sapienza, H. Thyrrstrup, S. Stobbe, P. D. Garcia, S. Smolka, and P. Lodahl, *Science* **327**, 1352 (2010), <http://science.sciencemag.org/content/327/5971/1352.full.pdf>.
- ³⁰ Z. Papi, E. M. Stoudenmire, and D. A. Abanin, *Annals of Physics* **362**, 714 (2015).
- ³¹ X. Li, D.-L. Deng, Y.-L. Wu, and S. Das Sarma, *Phys. Rev. B* **95**, 020201 (2017).
- ³² Y. Bar Lev, D. R. Reichman, and Y. Sagi, *Phys. Rev. B* **94**, 201116 (2016).
- ³³ W. De Roeck and F. m. c. Huveneers, *Phys. Rev. B* **90**, 165137 (2014).
- ³⁴ N. Y. Yao, C. R. Laumann, J. I. Cirac, M. D. Lukin, and J. E. Moore, *Phys. Rev. Lett.* **117**, 240601 (2016).
- ³⁵ A. Smith, J. Knolle, D. L. Kovrizhin, and R. Moessner, *Phys. Rev. Lett.* **118**, 266601 (2017).
- ³⁶ X. Li, S. Ganeshan, J. H. Pixley, and S. Das Sarma, *Phys. Rev. Lett.* **115**, 186601 (2015).
- ³⁷ R. Modak and S. Mukerjee, *Phys. Rev. Lett.* **115**, 230401 (2015).
- ³⁸ X. Li, J. H. Pixley, D.-L. Deng, S. Ganeshan, and S. Das Sarma, *Phys. Rev. B* **93**, 184204 (2016).
- ³⁹ S. Choudhury, E.-a. Kim, and Q. Zhou, ArXiv e-prints (2018), [arXiv:1807.05969 \[cond-mat.quant-gas\]](https://arxiv.org/abs/1807.05969).
- ⁴⁰ M. Schulz, C. A. Hooley, R. Moessner, and F. Pollmann, *Phys. Rev. Lett.* **122**, 040606 (2019).
- ⁴¹ B. Richard, *Annalen der Physik* **529**, 1700042, <https://onlinelibrary.wiley.com/doi/pdf/10.1002/andp.201700042>.
- ⁴² A. De Luca, B. L. Altshuler, V. E. Kravtsov, and A. Scardicchio, *Phys. Rev. Lett.* **113**, 046806 (2014).
- ⁴³ J. A. Kjäll, J. H. Bardarson, and F. Pollmann, *Phys. Rev. Lett.* **113**, 107204 (2014).
- ⁴⁴ S. D. Geraedts, N. Regnault, and R. M. Nandkishore, *New Journal of Physics* **19**, 113021 (2017).
- ⁴⁵ J. H. Bardarson, F. Pollmann, and J. E. Moore, *Phys. Rev. Lett.* **109**, 017202 (2012).
- ⁴⁶ M. Serbyn, Z. Papić, and D. A. Abanin, *Phys. Rev. Lett.* **110**, 260601 (2013).
- ⁴⁷ V. Khemani, S. P. Lim, D. N. Sheng, and D. A. Huse, *Phys. Rev. X* **7**, 021013 (2017).
- ⁴⁸ V. Oganesyan and D. A. Huse, *Phys. Rev. B* **75**, 155111 (2007).
- ⁴⁹ W.-J. Rao, *Journal of Physics: Condensed Matter* **30**, 395902 (2018).
- ⁵⁰ S. Bera, H. Schomerus, F. Heidrich-Meisner, and J. H. Bardarson, *Phys. Rev. Lett.* **115**, 046603 (2015).
- ⁵¹ S. Bera, T. Martyneć, H. Schomerus, F. Heidrich-Meisner, and J. H. Bardarson, *Annalen der Physik* **529**, 1600356 (2017), <https://onlinelibrary.wiley.com/doi/pdf/10.1002/andp.201600356>.
- ⁵² S.-H. Lin, B. Sbierski, F. Dorfner, C. Karrasch, and F. Heidrich-Meisner, *SciPost Phys.* **4**, 002 (2018).
- ⁵³ J. T. Edwards and D. J. Thouless, *Journal of Physics C: Solid State Physics* **5**, 807 (1972).
- ⁵⁴ D. J. Luitz, N. Laflorencie, and F. Alet, *Phys. Rev. B* **91**, 081103 (2015).
- ⁵⁵ M. Serbyn, Z. Papić, and D. A. Abanin, *Phys. Rev. B* **96**, 104201 (2017).

- ⁵⁶ J. L. C. d. C. Filho, A. Saguia, L. F. Santos, and M. S. Sarandy, *Phys. Rev. B* **96**, 014204 (2017).
- ⁵⁷ B. Villalonga, X. Yu, D. J. Luitz, and B. K. Clark, *Phys. Rev. B* **97**, 104406 (2018).
- ⁵⁸ M. Pouranvari and A. Montakhab, *Phys. Rev. B* **96**, 045123 (2017).